Journal of Sea Research 95 (2015) 22–35

Contents lists available at ScienceDirect

Journal of Sea Research

journal homepage: www.elsevier.com/locate/seares

Synoptic oceanography of San Jorge Gulf (Argentina): A template for Patagonian red shrimp (*Pleoticus muelleri*) spatial dynamics

Nora Gabriela Glembocki [a,*], Gabriela Noemí Williams [a], María Eva Góngora [c], Domingo Antonio Gagliardini [a,b], José María (Lobo) Orensanz [a]

[a] Cenpat-CONICET, Bvrd. Brown 2915, Puerto Madryn, Chubut (9120), Argentina
[b] Instituto de Astronomía y Física del Espacio (IAFE-CONICET), Pabellón IAFE-Ciudad Universitaria, C.C. 67-sucursal 28, Buenos Aires (1428), Argentina
[c] Secretaria de Pesca de la Provincia de Chubut, Rawson, Chubut, Argentina

ARTICLE INFO

Article history:
Received 7 November 2013
Received in revised form 1 September 2014
Accepted 19 October 2014
Available online 29 October 2014

Keywords:
Argentine Patagonia
Remote Sensing
SST
Chlorophyll *a*
Frontal Systems
Pleoticus Muelleri

ABSTRACT

An extensive series of high-resolution satellite images from the advanced very high-resolution radiometer (AVHRR) and the sea-viewing wide field-of-view sensor (SeaWIFS) was used in a synoptic oceanographic characterization of San Jorge Gulf (SJG, Argentine Patagonia), an area of great significance for marine conservation and commercial fishing. Remotely sensed information was combined with on-board observer's data and published information to investigate the role of distinctive oceanographic features in relation to the life cycle of the Patagonian red shrimp (*Pleoticus muelleri*), main target of the industrial fleet in SJG. Three frontal systems—North, South and Outer SJG—are characterized. The North and South SJG fronts are associated with shrimp reproductive aggregations during late spring and summer. While both function as spawning/nursery grounds, they differ from each other in many respects. The thermohaline South SJG front has its maximum expression during the winter, reflecting the influence of the low-salinity Magellanic Plume, while the thermal North SJG front develops during spring and summer as the water column becomes stratified in the central basin of the gulf. Wind-related downwelling inshore of the front prevails in the North SJG, and upwelling in the South SJG frontal area. Chlorophyll *a* is concentrated near the thermocline on the stratified side of the North SJG, and for that reason, it is not detected by remote sensors during the spring bloom and the summer but becomes apparent offshore from the location of the front when the thermocline deepens during the fall (May). In the South SJG front, Chl-a concentration is apparent inshore from the front all year-round, related in part to upwelling-mediated resuspension. The northern end of the outer front coincides in time and space with a recurrent non-reproductive aggregation of red shrimp between November and January and is presumably related to foraging. It is argued that keeping the North and South SJG frontal systems off-limits to fishing is a central precautionary requisite for the sustainability of the shrimp fishery.

1. Introduction

Over the last two decades, satellite-based technological developments have facilitated the macroscopic conceptualization of coastal ecosystems and the fisheries that they support (Klemas, 2012). This constitutes an opportunity in the case of coastal fisheries, often data-poor in terms of the fishery-independent data that support stock assessment and assessment-dependent management strategies. Remote sensing of coastal environments (Holman and Haller, 2013) and vessel monitoring systems (VMS) complemented with logbook or on-board observer programs (Gerritsen and Lordan, 2011), aided by the generalized use of geographic information systems (GIS) software, make it possible to identify and characterize major environmental drivers of stock spatial dynamics and the fishing process. This type of information is instrumental as support for spatially explicit strategies (Russo et al., 2014), e.g., reproductive refugia or marine zoning (Foley et al., 2010), that may prove effective in the face of uncertainty about stock size. Paradoxically, modern technology makes available the information needed for the diagnostic and management of fisheries considered "data-poor," largely located in the developing world.

The Patagonian red shrimp (*Pleoticus muelleri* (Bate, 1888), Fam. Solenoceridae) fishery offers an illustrative case. Landings from this lucrative industrial fishery, developed during the 1980s (Boschi, 1989, 1997), peaked in 2001 at 78,000 metric tons, fetching approximately U$S 375 million in exports revenues (Góngora et al., 2012). Fishing activity concentrates in San Jorge Gulf (SJG) and the adjacent shelf (Fig. 1). Surveys are carried on by national fisheries authority, but no formal stock assessment is conducted on a regular basis (Góngora, 2011). Management includes spatial and temporal closures, largely designed to prevent hake bycatch. It is generally held that the location of spawning grounds and migration routes are related to foraging and reproduction (Fernández et al., 2012; Roux et al., 2012), but the links

* Corresponding author.
E-mail address: glemboc@cenpat.edu.ar (N.G. Glembocki).

http://dx.doi.org/10.1016/j.seares.2014.10.011
1385-1101/

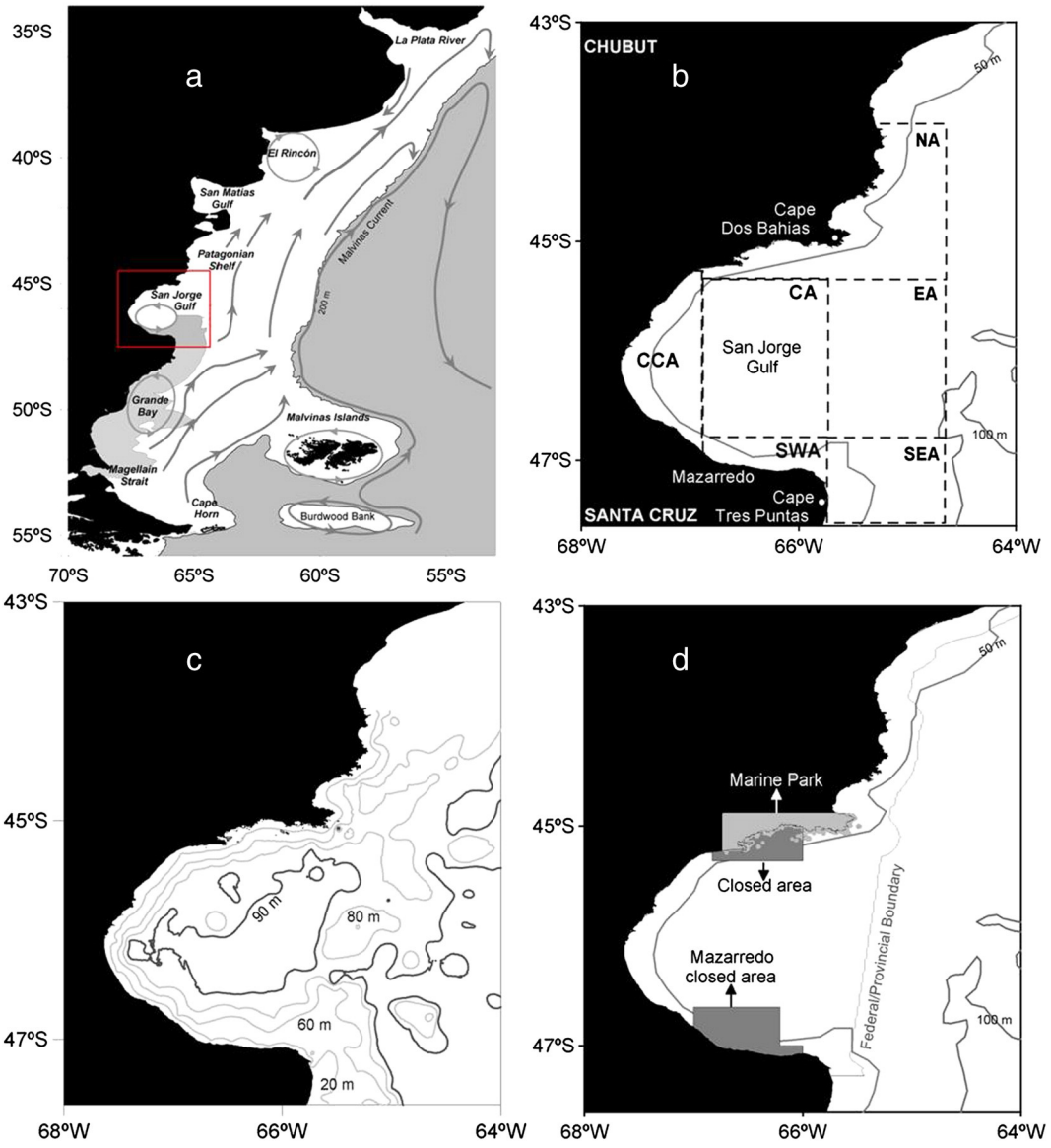

Fig. 1. Study region. (a) Southwestern Atlantic, showing main circulation patterns (arrows, after Palma et al. 2008) and the Patagonian Shelf (bound by the 200 m isobath); nearshore shading: areas of relatively low salinity of the Magellanic Plume; box: study area. (b) Partitions of San Jorge Gulf (SJG) used in the analyses (see text for explanation of acronyms). (c) Main bathymetric features of San Jorge Gulf. (d) Fisheries management jurisdictions and areas closed to fishing. (For interpretation of the references to colour in this figure, the reader is referred to the web version of this article.)

between stock spatial dynamics, effort allocation and regional oceanography are poorly understood.

High productivity in shelf ecosystems is often related to frontal systems, classical examples of "ocean triads": configurations favoring enrichment, concentration and retention (Bakun, 2010). Satellite remote sensing is particularly useful for the identification and characterization of the frontal systems that shape shelf ecosystems (Belkin et al., 2009). Thermal fronts are identifiable from sea surface temperature (SST) gradients, while, with due caveats, chlorophyll *a* (Chl-a) concentration has been used as a surrogate of phytoplankton concentration at the ocean surface. Major frontal systems from the Patagonian shelf, identified and characterized through the climatological analysis of remotely sensed SST and Chl-a concentration (Rivas and Pisoni, 2010; Rivas et al., 2006), support the productivity of regional fisheries (Acha et al., 2004; Alemany et al., 2014). Remote sensing has been combined with fisheries information to investigate the spatial dynamics of several resources, including scallops (Amoroso et al., 2011; Bogazzi et al., 2005) and hake (Ocampo Reinaldo et al., 2013; Williams et al., 2010).

Fishing and spawning grounds of the Patagonian red shrimp may be also related to shelf fronts, but specific linkages have not been investigated. Local fronts that recurrently develop in the SJG and its adjacencies have been usually subsumed in previous work as components of a broadly defined "Patagonian Tidal Zone" (Acha et al., 2004), an extensive region conformed by a string of localized frontal systems. A finer resolution is required, however, to investigate the role of oceanographic features in the spatial dynamics of specific inshore stocks (Gagliardini et al., 2004). On the other hand, information collected through an observer program (Góngora, 2011) indicates that the spatial pattern of effort allocation by the fleet shows high recurrence across years. Fishery-dependent data, if properly interpreted, often are more powerful than snapshot surveys for the purpose of identifying the spatial dynamics of populations showing ontogenetic migration. Combined investigation of climatologic patterns of environmental factors and of recurrent patterns of fishing intensity is potentially informative about the spatial dynamics of red shrimp in relation to major environmental features, but that type of scrutiny has not been yet conducted.

In this study, we used an extensive series of high-resolution images from the AVHRR sensor to identify frontal systems in the SJG and its adjacencies; climatologic characterization of the fronts was complemented by monthly averaged Chl-a concentration estimated from SeaWIFS images. Climatologic patterns of environmental variables were combined with aggregated information on the spatial dynamics of the fleet targeting Patagonian red shrimp. The emerging synopsis, combined with various pieces of existing information, provides a template to frame the spatial dynamics of the Patagonian red shrimp life history. Implications for management are discussed.

2. Study system

2.1. Study area

The SJG, a semi-open basin with an extension of 39,340 km^2, is located between 45°S (Cape Dos Bahías) and 47°S (Cape Tres Puntas), and between 65°30′W and the coast of Argentine Patagonia (Fig. 1). The central region of the basin, elliptical in outline, is well delimited by the 90 m isobath; maximum depth is 110 m near the center of the basin. Communication with the adjacent shelf spreads over approximately 250 km, at depths ranging from 90 m at the north and center to 50–60 m at the south end, where the basin is demarcated from the adjacent shelf by a pronounced sill know by fishermen as La Pared ("The Wall"). There are no rivers flowing into the gulf; precipitations are scarce (average: 233 mm yr^{-1} in Comodoro Rivadavia). Sediments from the central basin of the gulf, a depositional environment, are dominated by fine silt and rich in organic carbon derived from seasonally high phytoplanktonic primary production in the upper layer of the water column (Fernández et al., 2003, 2005, 2008); continental input is negligible. Consistently, oxygen concentration in near-bottom water is lowest in the central basin (Fernández et al., 2005).

The so-called Patagonian Shelf Water, including that of SJG, is a mixture of subantarctic water from the Cape Horn Current and low-salinity water from the Magellanic Plume (Fig. 1a). The latter, formed by the discharge from the Magellan Strait, extends along inner shelf of southern Patagonia (Palma and Matano, 2012), entering the southeast sector of SJG around Cape Tres Puntas (Cucchi Colleoni and Carreto, 2001; Fernández et al., 2005); in the adjacent shelf, the axis of the plume matches the 100 m isobath, which shifts offshore at the latitude of SJG. Modeling results indicate an anti-clockwise surface circulation in the southern half of SJG (Glorioso and Flather, 1995; Palma et al., 2004, 2008).

San Jorge Gulf presents particularly difficult management problems because it is exposed to environmental risks related to oil production: urban-industrial development of the Comodoro Rivadavia hub, prospective offshore drilling, and intense shipping activity (Nievas and Esteves, 2007). Oil production coexists with major fisheries targeting valuable shrimp, hake, scallops and king crab stocks (Góngora et al., 2012) and with areas of great significance for marine conservation because of the presence of reproductive aggregations and foraging grounds of many marine birds and mammals. This has been the main motivation for the creation of the first Argentine marine park along the north coast of the gulf (Yorio, 2001).

2.2. Red shrimp biology

The Patagonian red shrimp, a strictly marine species, has a broad latitudinal distribution range in the southwest Atlantic, from southeast Brazil to Argentine Patagonia. Boschi (1989, 1997) identified major concentration areas in the Argentine Patagonian shelf, between 43°S (Rawson) and 47°S (south end of SJG) (Fig. 2). With variants, conceptual models about the spatial dynamics (connectivity, migrations) of the Patagonian stock are based on a graphical model first introduced by Boschi (1989, his Fig. 14), in which the Rawson concentration area (Fig. 2) was thought to function as a major spawning ground. Red shrimp eggs are hyperbenthic; after hatching, there are several pelagic larval stages, followed by 4–6 mm long postlarvae that settle on soft bottoms (Iorio et al., 1990). Larvae were hypothesized to drift southward along the coast and metamorphose along the way to reach the nursery/wintering grounds of Bajo Mazarredo (Fig. 2) as pre-recruits. The cycle would be closed by a northward ontogenetic migration from Bajo Mazarredo to the Rawson spawning ground. Recent, more complex versions attach more significance as spawning grounds to other concentration areas (Góngora, 2011, her Fig. 2.1). Concentration of eggs and larvae has been observed during summer surveys in areas coincidental with major areas of shrimp aggregation (Fig. 2) (Fernández et al., 2012; Góngora et al., 2012; Moriondo-Danovaro, 2011). Starting in February and continuing during fall (March to May), subadults start a north-northeastward ontogenetic migration (Fig. 2), leaving the Bajo Mazarredo nursery and becoming vulnerable to the fishery. Reproductive maturity is reached at an age of one year (Fernández et al., 2012); maximum life-span is thought to be in the order of two years (Góngora, 2011).

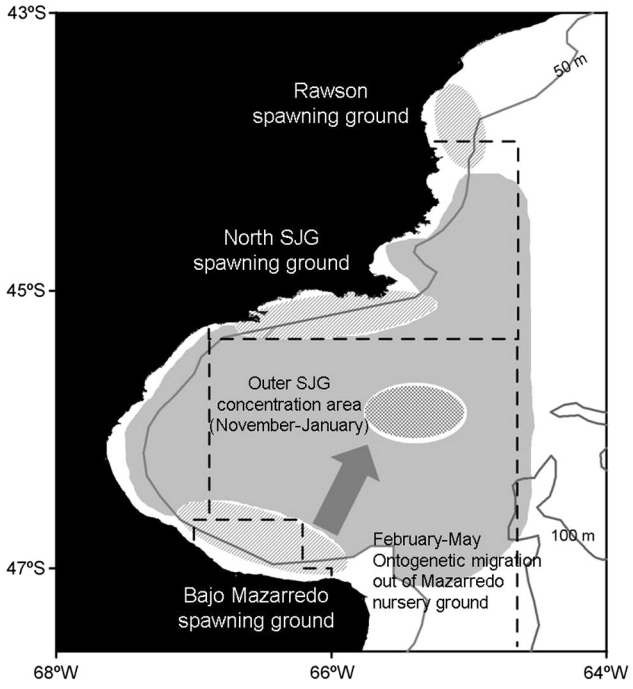

Fig. 2. Schematic of the distribution of Patagonian red shrimp (*Pleoticus muelleri*) in the study area (shaded), indicating documented spawning/nursery grounds (hatched), the outer gulf concentration area (November–January) and the axis of the ontogenetic migration out of Bajo Mazarredo (February–May, arrow).

2.3. The red shrimp fishery

The fleet targeting the Patagonian red shrimp stock has three components: (i) a fleet composed of 35 vessels 11–21 m long, which operates within the Chubut Province jurisdiction over the Rawson concentration area (43°S to 44°30' S) between September and March; (ii) a fleet of approximately 20 boats, 21–31 m long, that land the catch unprocessed and targets red shrimp opportunistically; and (iii) a fleet of double-rigged otter trawlers ("tangoneros") that, by 2011, consisted of 83 vessels 23–54 m long (Góngora, 2011). The latter operates in SJG under the two provincial jurisdictions and in the adjacent shelf, in federal waters, where it overlaps with an area designated for the protection of hake recruits, open to the red shrimp fleet on a seasonal basis. The tangonero fleet landed approximately 80% of the legal catch originated in the San Jorge and the adjacent shelf between 1991 and 2005 (Fischbach et al., 2006).

Argentina being a federal country by constitution, the red shrimp fishery operates under three jurisdictions: federal (offshore) and provincial (nearshore) (Fig. 1d).The nursery ground of Bajo Mazarredo (southern SJG, under Santa Cruz Province jurisdiction) has been permanently closed to fishing since 1985 (Fig. 1d); a sector of the northern fringe of the gulf (under Chubut Province jurisdiction), incorporated into a marine protected area, has been permanently closed since 2006 (Góngora et al., 2012). In order to address concerns about hake bycatch, both the provincial and federal fisheries administrations have introduced a complex and changing system of spatial and temporal closures (Góngora, 2011; Góngora et al., 2012). In 2001 the Chubut Province fishery administration introduced "mobile closures." Starting in 2003 the red shrimp fishing season has been regularly closed between October and December.

3. Materials and methods

3.1. Remote sensing data

3.1.1. Study area and image processing

The study area covers the entire San Jorge Gulf and the adjacent shelf (Fig. 1b). The region of interest was partitioned based on a preliminary analysis of seasonal maps of SST and Chl-a (Supplementary Materials SM1), prior information (Section 2.1) and basin topography. Six sectors were defined (Fig. 1b): Northern (NA), External or Eastern (EA), Central (CA), Central Coastal (CCA), Southeastern (SEA) and Southwestern (SWA).

All images were provided by Argentina's National Commission for Spatial Activities (CONAE), including the following:

3.1.1.1. SST images. A series of nine years (2000 to 2008) of high-resolution (1.1 km) images from the AVHRR sensor was used. SST was calculated through a method based on the "Split Window Technique" algorithm (McClain et al., 1985). SST calculation, further calibration, georeferencing and image analysis were performed using ERDAS Imagine 8.7 and R software (R Core Team, 2013).

3.1.1.2. Chl-a images. A series of seven years (2000–2006) of high-resolution (1.1 km) images of local area coverage (LAC) from the SeaWiFS sensor was used. Chl-a concentration was derived from the OC4 ocean color algorithm (O'Reilly et al., 1998, 2000) using SeaDAS (SeaWiFS Data Analysis System) version 4 (www.seadas.gsfc.nasa.gov).

All images were mapped to a WGS84 reference system (datum WGS84, ellipsoid WGS84) and co-registered using a calibrated coastline, and afterwards they were subset in order to circumscribe the study area (from 43°S, 67°10'12'' W to 45°30' S, 64°49'48'' W). A total of 360 SST and 510 SeaWiFS daily images were available from January 2000 to December 2006/2008 respectively.

Monthly mean images of SST and Chl-a were produced by arithmetically averaging all scenes available for each month, on a pixel-by-pixel basis, in order to obtain a series of twelve climatological images. Land and cloud pixels were flagged to zero and were not considered for the computations. The spatial resolution of the input images from both sensors (1.1 km) was kept in the resulting monthly mean images.

3.1.2. Analysis of remote sensing data

Monthly mean SST and Chl-a were calculated for each year of the time series using R software (R Core Team, 2013). Monthly SST averages were calculated using the five-day SST composites. Afterwards, the average of the monthly means for each series was calculated in order to obtain a climatological mean image for each month, a climatological image for each season, and finally, maps of mean SST and Chl-a which were the average of the whole time series for each parameter, each with its correspondent standard deviation (Supplementary Materials SM1).

The SST stationary signal as well as the annual harmonics for each area, from 12 climatological monthly SST composites, were calculated using least square fitting (Beron-Vera and Ripa, 2000). Regardless of the semiannual component, the fit reduced to:

$$\mathrm{SST}(x,t) = \mathrm{SST}_1(x) + T_1(x)\cos[w(t-t_0)]$$

where SST_0 is the mean SST temporal value, T_1 is the annual harmonic amplitude, w is the frequency ($w = 2.\pi/12$) and t_0 is the annual harmonic phase. In this case t_0 indicates the time of the year with maximum SST.

In order to detect frontal zones or other areas with abrupt changes in SST, gradients (°C. km^{-1}) were calculated from each monthly SST image by applying a Sobel operator in a 5×5 pixel window (Simpson, 1990). The Sobel operator consists of two 5×5 pixel convolution masks, which are used to calculate two images containing approximations for derivatives (in west-east and north-south directions) and assuming that there is an underlying continuous intensity function. At each pixel of the image, gradient magnitudes are computed and the results show how "abruptly" or "smoothly" the image changes at that pixel. Maps of seasonal climatological SST fronts were obtained by applying a threshold criterion that allowed the distinction between gradient values that corresponded to SST fronts and background values, which indicate the natural variability of the SST field among pixels. The separation between frontal pixels and background was performed following Bava (2004), who used the distribution of frequencies of pixels in the seasonal SST images. Those pixels with frequencies below 10% of the total were considered as frontal.

3.2. Fishery data

On-board observer programs were implemented by provincial fisheries administrations since 2000/2001 to monitor the red shrimp fishery. Data for the period 2001–2008 from the Chubut Province observer program (Góngora, 2011) were used to characterize the spatial allocation of effort by the fleet targeting red shrimp in SJG. Records for each fishing haul include vessel ID, observer ID, date, haul duration, initial haul position (latitude and longitude) and shrimp catch. Cover of the tangonero fleet ranged from 7.5% to 15%, depending on the year. Year 2005 was excluded from the analyses because unusual temporal and spatial closures were implemented in response to low shrimp abundance. The data set consisted of 45,434 hauls, made during 337 fishing trips and 8,155 fishing days. Fishing intensity was calculated on a monthly basis as the number of hauls (initial position) per $2' \times 2'$ cell. Complete vessel monitoring system (VMS) records for the tangonero fleet were obtained from the national fisheries authority for the period 2006–2008 and used to determine if data from the observer program had the appropriate spatial coverage of the region of interest. It was considered that speed records in the range of 2 to 5 knots (typical for trawling) correspond to fishing time. Spatial distribution of records from the observer program and VMS were compared for that period; no apparent biases were detected in the spatial and temporal coverage of the observer program (Góngora, 2011). Special care was taken to contemplate temporal and spatial closures (Section 2.3) in the interpretation of observed patterns of fishing intensity. Observer program data were chosen over VMS data because they correspond to discrete fishing events, more amenable than VMS records to testing the distribution of effort in relation to environmental variables. CPUE was not used in the analyses because it has not yet been standardized in the data base from the fisheries authority. Besides, effort allocation is expected to be more reflective of recurrent patterns of distribution than the abundance index, prone to higher year-to-year variation.

3.3. Relationship between fishing effort and oceanographic features

The region where the fleet operates was partitioned in two sectors (north and south) (Fig. 2). Areas closed to fishing (Robredo and Mazarredo) and the shelf west of 64.7°W were excluded. Polygons

bounding fronts were constructed for each month. Fronts were defined by a threshold SST gradient value of 0.04 °C km^{-1} (Bava, 2004; Williams et al., 2010). Analyses were conducted separately for each sector and month. The relation between fishing intensity and SST, chl-A and frontal areas was investigated with the method developed by Perry and Smith (1994), in which the null hypothesis of a random association between fish distribution and habitat conditions is tested. The method can be used to investigate the distribution of fishing intensity as well. The general frequency distribution of a habitat variable (SST, Chl-a, ΔSST) is characterized by means of its empirical cumulative distribution function (ecdf):

$$f(t) = \frac{1}{n}\sum_{i=1}^{n} l(x_i)$$

with the indicator function

$$l(x_i) = \begin{cases} 1, & \text{if } x_i \le t \\ 0, & \text{otherwise} \end{cases}$$

where n is the total number of cells and t represents an index, ranging from the lowest to the highest value of the habitat variable at a step size appropriate for the desired resolution. Next, fishing intensity (as number of hauls per cell) is associated with the environmental as a weight in a cumulative distribution function,

$$g(t) = \frac{1}{n}\sum_{i=1}^{n} y_i l(x_i)$$

where y_i represents the frequency of occurrence of hauls in each cell (calculated as the number of hauls per cell divided by the total number of hauls). All calculations were done on a monthly basis. Strength of the association between fishing activity and habitat variables is tested by assessing the difference between the two curves, $g(t)$ and $f(t)$. The test statistic is constructed by calculating the maximum absolute vertical distance between them, which is similar to the Kolmogorov-Smirnov test for comparing ecdf's.

A chi-square goodness of fit test (Zar, 1999) was applied to test the null hypothesis of no difference in the distribution of fishing intensity between front polygons and the rest of the region where the fleet operates. Following Alemany et al. (2014), the observed frequency of hauls inside and outside the frontal polygons was compared with the frequencies expected if effort allocation were proportional to the area of the two regions. Regions of interest were defined so as not exceed the positive area (Woillez et al., 2007), in order to avoid inflation of the test statistic.

4. Results

4.1. Temporal evolution of mean SST and Chl-a concentration

In order to show the temporal variability of SST and Chl-a concentration, the climatological monthly mean spatial values of both variables were calculated for each of the six sub-areas. SST showed a clear seasonal cycle (Fig. 3); the annual cycle explained more than 99% of the variance (Table 1). In this case, the change of phase corresponded to the moment of the year when SST was highest, at the beginning of February (t_0 = 2.08, 17.10 °C) in most of the gulf and around mid-February in the eastern area (t_0 = 2.29, 15.17 °C). Surface water was warmest in the coastal-central, central and northern areas (13.13 °C, 13.48 °C and 13.65 °C, respectively; Table 2). The eastern and southwestern areas showed the lowest and the highest thermal amplitudes respectively (3.12 °C and 4.00 °C). Lowest mean and minimum SST corresponded to the southeastern and southwestern areas.

There was a general tendency towards low concentrations of Chl-a in winter and high concentrations between October and April (Fig. 3; Table 3). The absolute minimum values were found in the southwest (0.42 mg m^{-3}) and the absolute maxima in the central and coastal-central areas (3.11 mg m^{-3} y 3.42 mg m^{-3}, respectively), while the minimum mean values occurred in the southeastern (1.31 mg m^{-3}) and the maximum mean values over the coastal-central (1.84 mg m^{-3}) and southwestern (1.62 mg m^{-3}) areas. These results show that there could be a progression in the moment of occurrence of the autumn bloom, moving from the deeper parts of the gulf (to the east) towards the coastal zone. Over the eastern area, the peak occurs between February and March; in the northern, southeastern and central areas in March, and in the coastal-central area in April. It is not the same with the spring bloom, which occurs in October over all the areas except for the east and the southeast, where it begins in November. Table 4 describes, in detail, the annual cycle of Chl-a concentration at each particular area.

4.2. Thermal gradients

Seasonal and monthly gradient maps of SST give a general indication of the structure, extent, variability and intensity of thermal fronts in SJG. Since such maps were produced from a series of 9 years of AVHRR images, only those frontal zones that occur recurrently through time are likely to be captured by monthly and seasonal averages. Three fronts were clearly discernible during summer: South, Outer and North SJG, all characterized by gradients of 0.05 °C–0.15 °C km^{-1} (Fig. 4a). In autumn (Fig. 4b), SST was homogeneous across the whole gulf; consequently, there were no significant thermal gradients. The South SJG thermohaline front was most developed during winter, along the coastal zone around the cape (Fig. 4c, southeastern and southwestern areas), indicating the difference in SST between the relatively warm inner waters of SJG and the colder waters of the Magellanic Plume entering the gulf from the south. The North SJG thermal front, which develops in spring (Fig. 4d) and is strongest during summer (Fig. 4a), is a consequence of the tidal mixing generated by the topography of the coast. The Outer SJG thermal front develops during spring (Fig. 4d), reaching its maximum spread in summer (Fig. 4a).

High apparent concentration of Chl-a is observed inshore of the South SJG front all year-round (Supplementary Materials Fig. SM1.4). On the northern coast of the gulf, concentration of Chl-a is high only during summer and along the narrow fringe inshore of the North SJG front (Supplementary Materials Fig. SM1.4a). During fall, a bloom occurs recurrently in May offshore of the North SJG front summer position; this phenomenon is clearly observable in autumn climatologies (Supplementary Materials Fig. SM1.4b). High concentration of Chl-a clearly matches the Outer SJG front during summer. Starting during mid spring (November through January) a bloom develops recurrently at the northern end of the front, centered in the eastern area (Supplementary Materials, Fig. SM1.4d, EA).

4.3. Fishing intensity

Three months—December, February and August—were selected for detailed presentation of results because of them being demonstrative of significant patterns of effort allocation (Fig. 5). Information for the other months is presented under Supplementary Materials (SM2). Spatial effort allocation by the Chubut Province tangonero fleet generally tracked the spatial dynamics of red shrimp as currently understood.

In February, effort concentrated in the North and South SJ frontal areas (Fig. 5f). In the south the fleet converged on the eastern boundary of the Mazarredo closure (off Cape Tres Puntas), targeting subadults as they exited the nursery ground and started migrating towards the northeast along a corridor coincidental with the main axis of the Outer SJG front, bound by the slopes of the sill (Fig. 5f). Most of the effort was allocated within the frontal area (Fig. 6f; Table 5), coinciding with high Chl-a concentration (Figs. 5e and 6e) and the warmest part of the frontal area (16.5 °C–17.5 °C; Figs. 5d and 6d). While the fleet continues targeting outmigration shrimp through May, the strong,

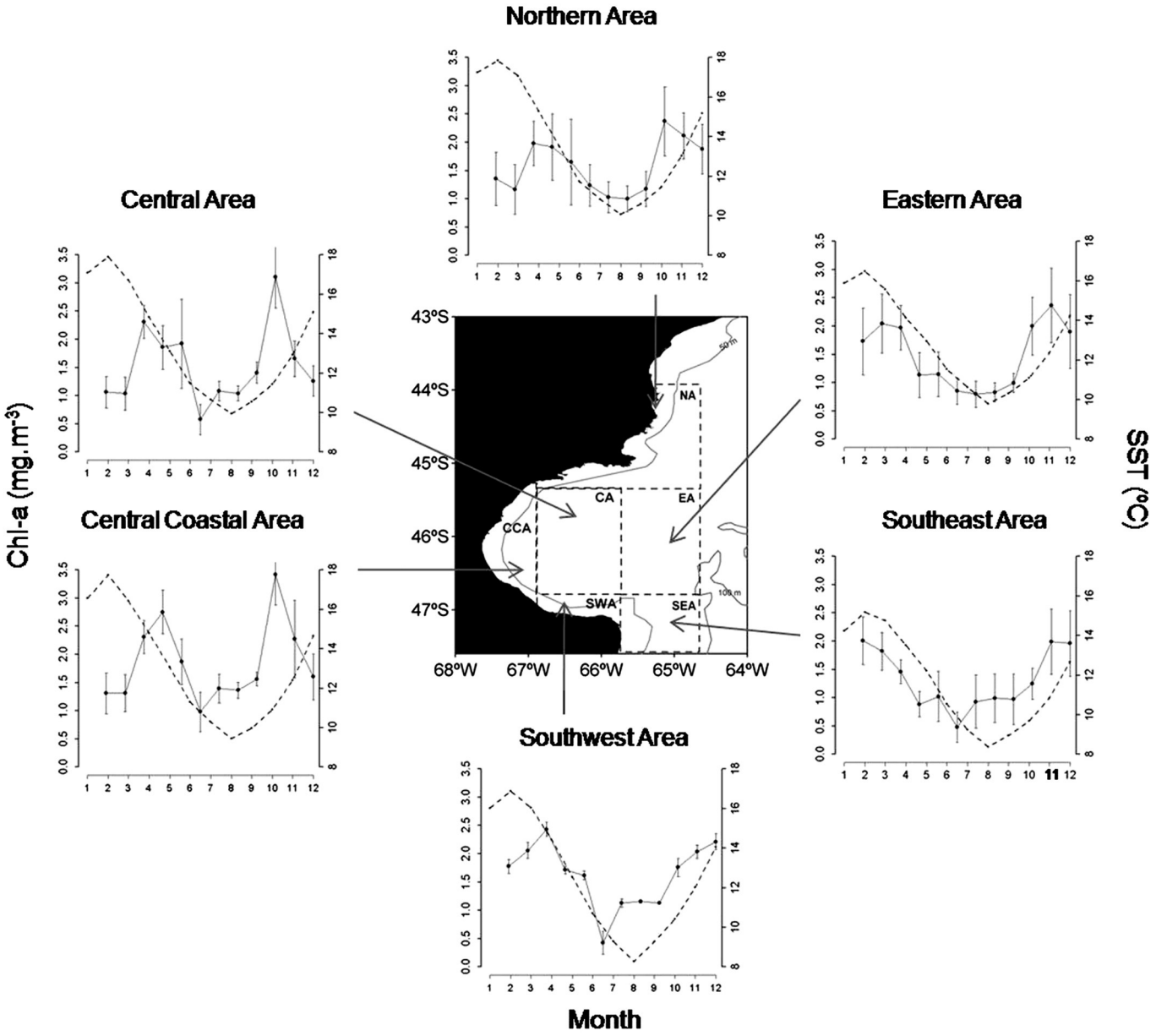

Fig. 3. Climatological annual cycles of SST and chlorophyll *a* in San Jorge Gulf, by partitions.

front-associated effort concentration observed in February gradually faded away (Supplementary Materials SM2). Only a few boats operated in the northern gulf in February, catching large shrimp from the escapement of the previous fishing season. Effort was significantly associated with the North SJG frontal region (Figs. 5f and 7f; Table 5), strongly overlapping areas of high Chl-a concentration (Fig. 7e) but not clearly related to SST (Fig. 7d). Effort concentration in the north persisted through April (Supplementary Materials SM2).

Frontal systems vanished during the fall (April–May). During the winter (June–September), effort was increasingly dispersed over open areas of SJG and the adjacent shelf (Fig. 5i; Supplementary Materials SM2), expanding offshore into federally managed waters in case of not

Table 1
Parameters of the annual model of the thermal cycle for the climatological mean values over each area (based on monthly values).

Area	SST_0	T_1	w	t_0	r^2
NA	13.65	3.81	0.52	2.05	0.99
CA	13.48	3.74	0.52	1.96	0.99
EA	12.92	3.12	0.52	2.06	0.99
CCA	13.13	3.82	0.52	2.06	0.99
SEA	11.69	3.22	0.52	2.29	1.00
SWA	12.50	4.00	0.52	2.05	1.00
GSJ	13.03	3.57	0.52	2.08	0.99

Table 2
Descriptive statistics for the mean climatological values of SST in each area (based on monthly values).

Area	Mean	Min	SD	Max	Month max	Month min
NA	13.65	10.07	2.80	17.85	February	August
CA	13.48	9.94	2.79	17.91	February	August
EA	12.92	9.80	2.32	16.48	February	August
CCA	13.13	9.44	2.85	17.74	February	August
SEA	11.69	8.37	2.39	15.17	February	August
SWA	12.50	8.28	2.96	16.88	February	August
GSJ	13.03	9.56	2.65	17.10	February	August

Table 3
Descriptive statistics for the mean climatological values of chlorophyll *a* over each area (mg m^{-3}, based on monthly values).

Area	Mean	Max	Min	SD	Month max	Month min
NA	1.57	2.35	1.00	0.46	October	August
CA	1.53	3.11	0.57	0.69	October	June
EA	1.48	2.37	0.80	0.57	November	July
CCA	1.84	3.42	0.97	0.71	October	June
SEA	1.32	2.01	0.48	0.52	January	June
SWA	1.62	2.43	0.42	0.57	March	June
SJG	1.54	2.53	0.89	0.51	October	June

being a hake-related closure. The extension of the positive fishing area was largest by August–September (Fig. 5i). Association with fronts vanished in both the north and south regions of SJG (Table 5; Figs. 5i, 6i and 7i). This was particularly noticeable in the south SJG, where the South SJG thermo-haline front developed during the winter but virtually no effort was allocated within polygon boundaries (Figs. 5i and 6i). Effort concentrated in areas with relatively high SST (>9 °C in the south, >10 °C in the north; Figs. 6g and 7g) and low Chl-a concentration (<1 mg m^{-3}; Figs. 6h and 7h).

During the spring (October–December), the trend described above reversed, as effort concentrated on three areas (Fig. 5c): (i) a fishing ground located at the entrance of the gulf, around 45°S; (ii) the North SJG front; and (iii) a fishing ground off Rawson, north of SJG. Effort allocation to the south sector continued to be negligible through January (Figs. 5c and 6a–c). Ground i appears to be associated with a topographical elevation of the sea bed bound by the 80 m isobath (Fig. 1c), coincidental with high Chl-a concentration in late spring (November-December, Fig. 5b). We do not further consider this transient aggregation. It could not be observed since 2003, when a seasonal closure (October-December) was introduced. The fishing ground off Rawson, a sink presumably sustained (at least in part) by migrants originating in the spawning grounds of SJG, is outside our focal region.

By late spring and early summer (December–January), while effort deployment within the North SJG front was significant (Table 5), there was substantial allocation outside the boundaries of the climatological polygon (Figs. 5c and 7c), probably a result of year-to-year variation in a narrow and highly dynamical frontal region. Effort concentrated in regions of relatively high Chl-a concentration (>1.7 mg m^{-3}; Fig. 7b), but largely irrespective of SST (Fig. 7a).

5. Discussion and conclusions

Three recurrent fronts—South, North and Outer—were identified and characterized as a result of our inquiry, based on climatologic monthly averaged SST obtained from an extensive series of images from the AVHRR sensor, and of Chl-a concentration from the SeaWIFS sensor. While we acknowledge the existence and significance of year-to-year and within-month variability in the variables examined, our objective was to describe the broad, average climatologic patterns associated with the frontal systems that appear to play a role in red shrimp spatial dynamics, as inferred from the behavior of the fleet and several pieces of biological information. Variability at finer time resolution will be addressed in forthcoming contributions, framed in the context defined by this study. Below we discuss our findings together with existing information on red shrimp biology.

5.1. South SJG thermohaline front

The observed winter SST minima at the southeastern sector of SJG can be explained by the influence of relatively cold, low salinity water from the Magellan Plume (Palma and Matano, 2012). A thermohaline front, made evident by summer and winter SST gradients, results from penetration of the plume, together with the turbulent mixing generated by tidal currents (Acha et al., 2004; Bogazzi et al., 2005). This sector showed the widest thermal amplitude of the study region; near-shore water temperature reaches regional minima below 6 °C during the winter. The reason is that the permanent, tide-originated turbulent mixing distributes heat flow over the entire water column, thus impeding stratification (Rivas, 2010; Rivas and Pisoni, 2010; Tonini et al., 2006). Vertical mixing in this sector is well captured by the Simpson-Hunter parameter, calculated by means of hydrodynamic models (Glorioso and Flather, 1995; Palma et al., 2004); here tidal energy flow is among the highest in the world (Tonini et al., 2006).These processes also explain the later occurrence of the annual SST maximum (mid to late February) relative to other sectors of SJG. Consistently with the thermal cycle, the cycle of Chl-a concentration follows a pattern typical of waters not seasonally stratified, characterized by relatively low variability and high summer concentration. High apparent year-round Chl-a concentration was observed in the coastal zone at the southeast of SJG (shallower than 50 m), inshore from the South SJG front. The signal may be amplified by sediment resuspension due to mixing resulting from interaction of topography with wind and tides (Rivas et al., 2006). Modeling results indicate upwelling driven by dominant strong winds along the south and southwest coasts of SJG (Tonini et al., 2006) which, combined with the primarily silty nature of sediments from the Bajo Mazarredo region (Boschi, 1989; Fernández, 2006), define a likely scenario for protracted sediment resuspension. Persistence of a strong Chl-a signal, however, extends to the east, around Cape Tres Puntas and southward alongshore, where sediments are composed of coarse (gravel) to very coarse fractions (Fernández, 2006; Fernández et al., 2003; Ponce et al., 2011). In fact, Chl-a concentration in superficial sediments showed regional maxima in this sector during spring and winter (Fernández et al., 2008). During winter, mean total organic carbon was highest and the C:N ratio was lowest (indicative of high food quality), reflecting the lack of a thermocline (Fernández et al., 2005). While Chl-a concentration was low in the water column, resuspended material could also be a significant trophic input for stocks of benthic or demersal invertebrates (Grant et al., 1997). An upwelling zone in

Table 4
Outstanding features of annual cycle of chlorophyll *a* concentration in areas of San Jorge Gulf (shown in Fig. 1b).

Area	Background/minima	Blooms	Maxima (mg m^{-3})
North (NA)	Begins to decrease towards late autumn and stays low until early spring.	Spring (October) and autumn (March) peaks, as in EA, but the autumn peak occurs one month later.	Spring bloom: 2.35
East (EA)	Low between mid-autumn and early spring.	Two peaks: spring (November) and a smaller one at the end of summer (February-March)	Spring bloom: 2.37
Coastal Central (CCA)	Lowest in winter; drops during summer to levels comparable to those of winter.	Peaks in spring (October) and again in autumn (April), later than over the other areas.	Spring bloom: 3.42
Central (CA)	Similar to CCA, with minimum concentrations in winter and summer	Two peaks, one in spring (October) and another one in autumn (March)	Spring bloom: 3.11
Southeast (SEA)	Low concentrations persisted throughout the year.	Slight increase between November and March.	Summer: 2.01
Southwest (SWA)	Minimum in winter.	Rising in spring (October) and reaching its maximum in autumn (March). No second peak detected, as chlorophyll *a* levels remain constant during the whole summer.	Autumn bloom: 2.43

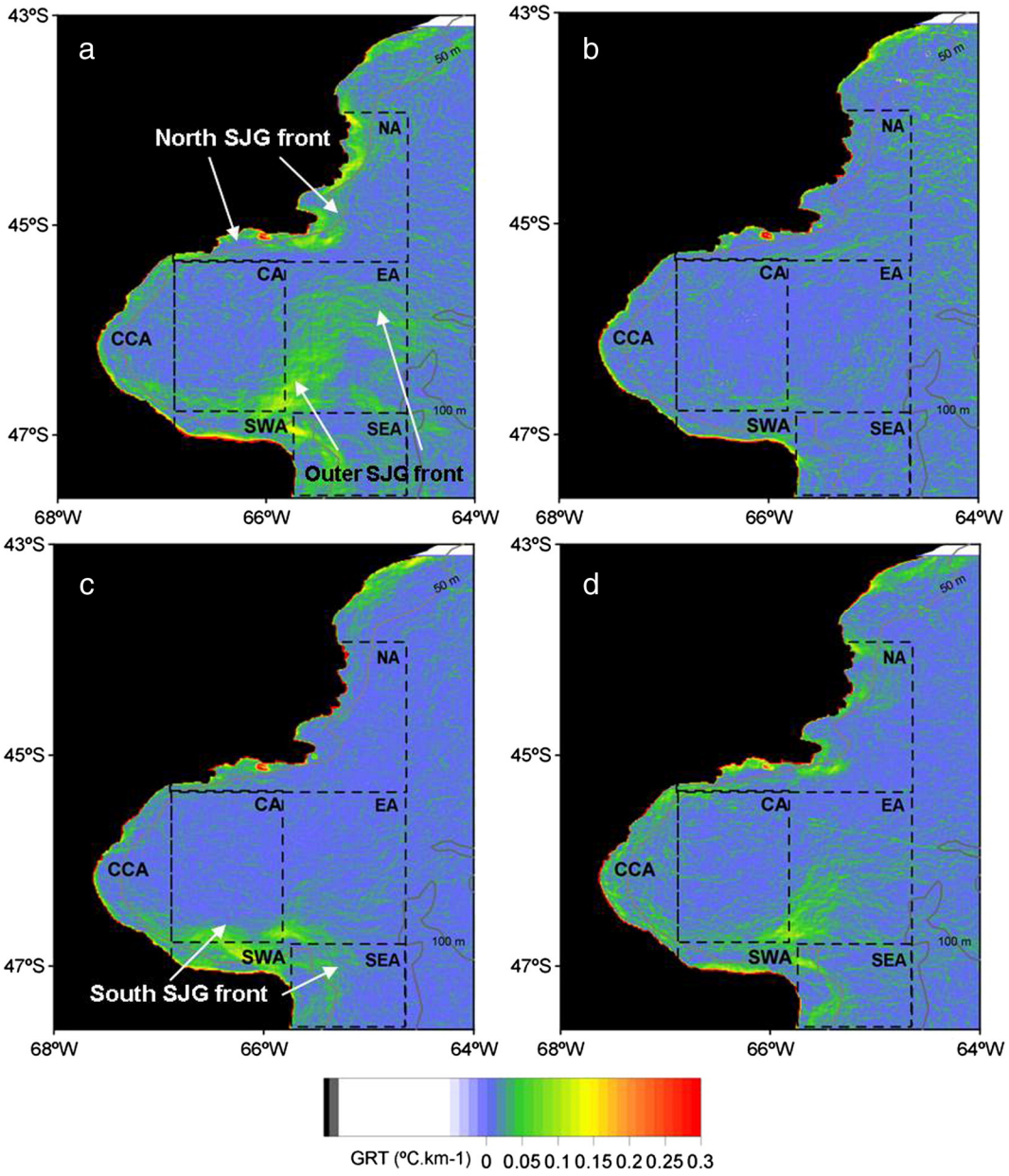

Fig. 4. Location of seasonal climatological thermal gradients (°C km^{-1}). (a) Summer. (b) Autumn. (c) Winter. (d) Spring.

the Bajo Mazarredo area, bound by the South SJG front, is likely to favor larval retention, while high concentration of suspended particulate matter, facilitated by vertical mixing, is indicative of favorable conditions for juvenile red shrimp overwintering.

5.2. Outer SJG thermal front

To the northeast of Cape Tres Puntas, the Outer SJG thermal front develops during spring, reaching its maximum spread in summer. During spring and summer, the front separates the stratified waters of the inner gulf from the vertically mixed waters overlaying the southeastern area (Carreto et al., 2007). During fall and winter the water column is homogeneous on both sides of the frontal system. The main axis of the Outer SJG thermal front (southwest–northeast direction), coincidental with the La Pared sill, is matched by the ontogenetic migration of red shrimp moving out of the Bajo Mazarredo ground (closed to fishing since 1985) and becoming vulnerable to the tangonero fleet. The migration route is also coincidental with the general direction of residual circulation over the outer gulf and adjacent shelf (Palma et al., 2004, 2008), which could facilitate transport given that migrating shrimp swim in midwater at nighttime (Roux et al., 2012). A localized area of high Chl-a concentration that develops recurrently at the northern end of the Outer SJG, between November and January, corresponds to "frontal area 7" of Rivas (2006, his Fig. 3). This ostensible feature is also shown (albeit not discussed) by Cucchi Colleoni and Carreto (2001, their Figs. 7d, 8d and 9d) and Carreto et al. (2007, their Fig. 14). The same area was highlighted by Boschi (1989, his Fig. 1, zone 2) as one among five grounds of concentration of Patagonian red shrimp and fishing intensity. Effort allocation data highlight this as an area of high fishing intensity before 2003 (when a seasonal closure was introduced) between November and January, precisely matching (temporally and spatially) the Chl-a concentration signal. Biological information collected by the observers program and surveys of eggs and larvae indicate that this is not a shrimp spawning/nursery ground. Unnoticed before, this concentration area is located on a topographically elevated area bound by the 80 m isobath. High productivity may be related to interaction between

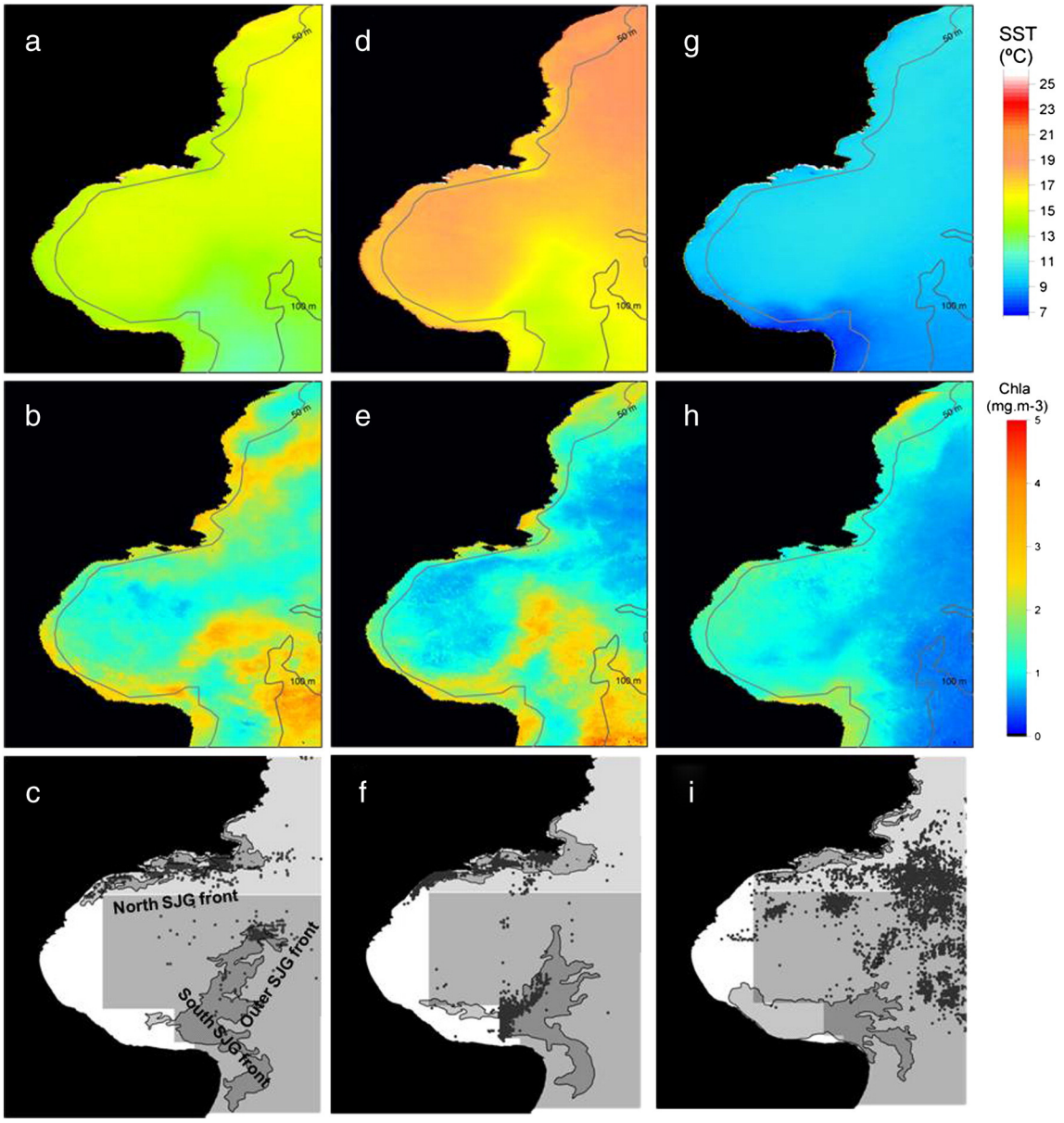

Fig. 5. Correspondence between spatial effort allocation (fishing intensity) and significant oceanographic features during representative months (December, February and August). Top row: distribution of climatological SST (2000–2008); middle row: ibid., chlorophyll *a* (2000–2006), lower row: front polygons and location of fishing events (2001–2003 for December, 2001–2008 for February and August).

this feature and circulation. Transient shrimp concentration in this area during late spring and early summer may be related to foraging.

5.3. North SJG thermal front

The North SJG thermal front develops during spring and summer, at the boundary between the stratified waters of the central area and the vertically mixed coastal waters. Such mixing is the result of the interaction between tidal currents and coastal topography (Gagliardini et al., 2004; Palma et al., 2004; Rivas and Pisoni, 2010; Tonini et al., 2006). The consequent dissipation of energy explains the relatively late occurrence of the annual SST maximum (e.g., as compared to the central area), estimated for early February. Modeling results indicate that down-welling caused by the strong winds from the west quadrant may be significant along the north coast of SJG (Tonini et al., 2006), inshore from the front. Spring and fall maxima of Chl-a concentration are indicative of phytoplanktonic blooms, a cycle typical of temperate regions, where spring blooms have been extensively studied. It is generally accepted that they are caused by a combination of vertical stratification and increasing solar radiation after winter replenishment of nutrients by convectional mixing (Evans and Parslow, 1985). Low sea-surface concentration of Chl-a during summer is likely to be the result of nutrient depletion in the euphotic zone (Akselman, 1996; Carreto et al., 2007; Cucchi Colleoni and Carreto, 2001), and of higher consumption of phytoplankton by zooplankton (Boschi, 1989). A deep chlorophyll maximum (DCM) extends over most of the central basin during summer at 40–60 m depth, matching the thermocline (Cucchi Colleoni and Carreto, 2001). The frontal system coincides, spatially and seasonally, with a major concentration of spawning shrimp and of fishing intensity. The fleet targets large, mature shrimp between November and March (Góngora, 2011). Paradoxically, the Chl-a concentrations detected in satellite images are low along the frontal area during the spawning period. At that time, Chl-a is concentrated at the DCM, on the stratified side of the front. It is thus suggestive that

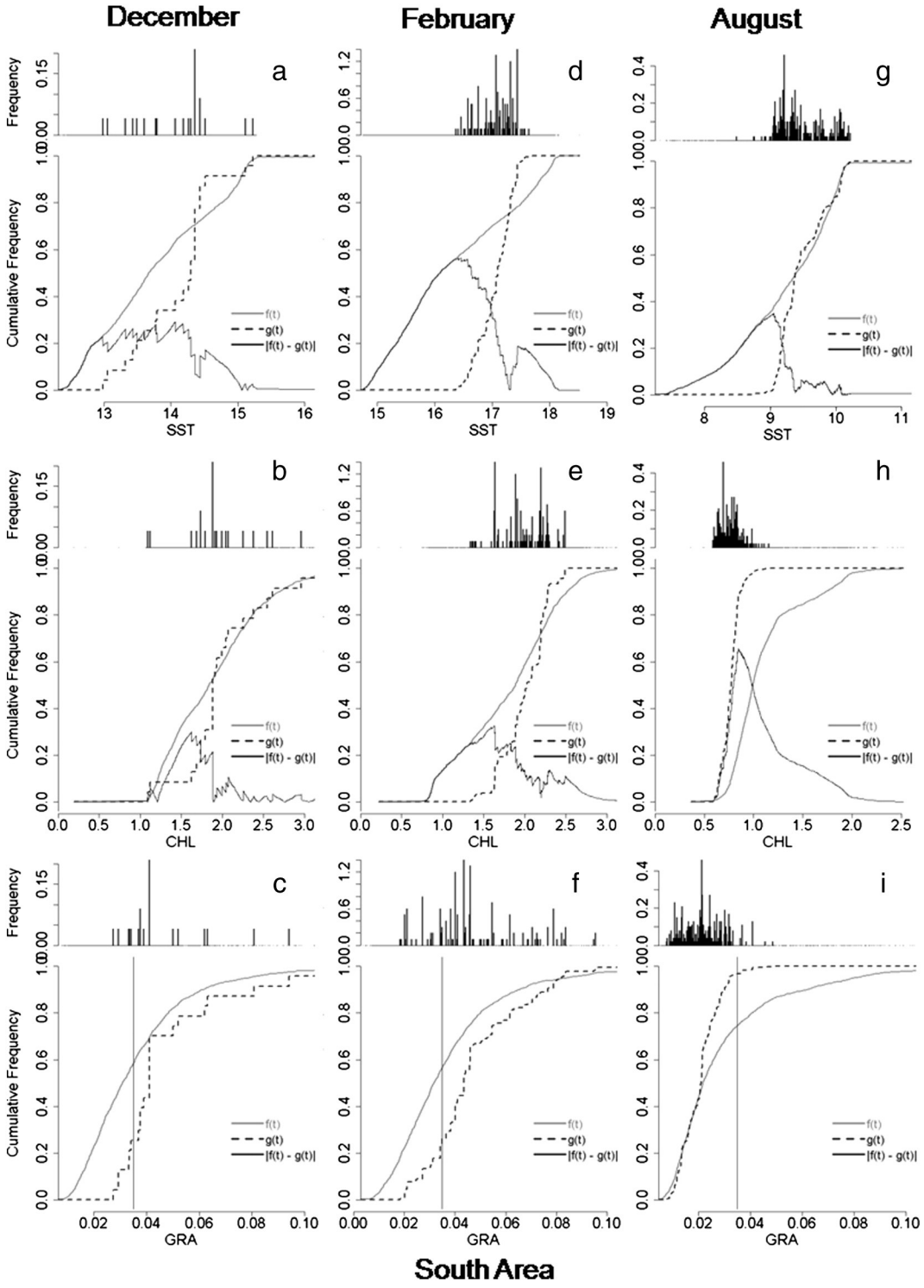

Fig. 6. Relation between environmental factors and fishing intensity, south sector of San Jorge Gulf; December, February and August (2000–2008 averages). Main panels: normalized empirical cumulative distributions of environmental factors (ecds), ecds weighted by fishing intensity and absolute difference between the two. The difference between the two curves is statistically significant in all cases. Top row: sea surface temperature (SST), middle row: chlorophyll a (Chl-a) concentration, bottom row: SST gradient steepness (ΔSST). The histogram at the top of each panel shows the frequency distribution of fishing effort for bins of the environmental factor.

maximum concentration of red shrimp larvae have been observed near the thermocline (Fischbach, 1993).The DCM is a likely source of larval food in stratified zones, where nutrients are depleted in the photic zone. A short lived but intense bloom in May, south of the front location and followed in June by localized Chl-a depletion, may be related to the deepening of the thermocline. While spring blooms are reasonably well understood in temperate regions, autumn blooms are less well studied. Modelling results indicate that they are transient states between summer and winter quasi-equilibria states and are expected to depend on the rate at which the thermocline deepens (Findlay et al., 2006). It is interesting to notice that this localized autumn bloom occurs offshore of the North SJG frontal area, while spring or summer blooms in most coastal sectors of the region occur on the colder and shallower side of the surface thermal fronts. The latter is the case of areas 4, 5, 6 and 8

Table 5
Expected and observed fractions of effort deployed within frontal areas of San Jorge Gulf, north and south sectors, by month (aggregated data for period 2000–2008). Total area of north sector: 1,462,919 ha, south sector: 3,510,572 ha. Chi-square critical value ($\alpha = 0.01$) is 6.63. No fronts were observed in April; in May a front developed in the south sector only.

				Frontal hauls			
	Month	Total no. of hauls	Frontal area	% Expected		% Observed	Chi-squared
North area	January	657	453657	31.15	<	71.84	507.21***
	February	3487	253825	32.52	<	60.77	1267.95***
	March	2351	88232	6.08	<	26.03	1638.33***
	April	517	0	–	N/A	–	–
	May	648	0	–	N/A	–	–
	June	543	34844	2.40	<	5.16	17.54***
	July	1038	118828	8.20	>	3.47	30.86***
	August	1561	144086	9.92	>	1.92	111.67***
	September	1777	74533	5.14	>	1.24	55.57***
	October	2688	204267	14.12	<	28.01	427.86***
	November	2549	130919	9.02	<	20.40	402.31***
	December	1821	209336	16.03	<	49.31	2788.05***
South area	January	123	776360	22.21	>	1.63	30.15***
	February	979	534606	16.69	<	60.16	1331.05***
	March	3062	347029	9.94	<	65.25	10461.91***
	April	4248	0	–	N/A	–	–
	May	5438	150387	4.33	>	0.81	162.81***
	June	3903	245153	7.05	>	0.64	244.65***
	July	2864	324988	9.33	>	1.78	193.08***
	August	2274	358355	18.25	>	0.66	471.68***
	September	2736	230720	6.61	>	0.44	168.72***
	October	2145	302156	8.58	NS	7.83	1.51
	November	812	274779	17.84	<	63.79	1169.64***
	December	263	585571	17.33	<	53.99	246.86***

identified by Rivas (2006, his Fig. 3), included in our north, southwest and southeast sectors (Table 4).

5.4. Connectivity between frontal systems

Before the spawning grounds of SJG were documented, Boschi (1989) hypothesized a post-larval return from the Rawson spawning ground to the Bajo Mazarredo nursery ground. This is highly unlikely given the current understanding of circulation in the inner shelf between 43°S and 48°S (Palma et al., 2008). Under the current hypotheses of connectivity between major spawning grounds (Góngora, 2011), the inner gulf is the necessary scenario for post-larval drift from the north SJG spawning ground to Bajo Mazarredo, the major spawning/nursery ground at the south of the gulf. Southward drift along the west coast would be favored by a counterclockwise circulation in SJG (Glorioso and Flather, 1995; Palma et al., 2004, 2008). The latter, however, has not been validated by field observation. Besides, it has been well documented that penaeoid shrimp larval and post-larval transport can be partly controlled by complex behavioral responses to tidal currents (Criales et al., 2011; Rothlisberg et al., 1995; Wenner et al., 2005), which are strong in SJG (Tonini et al., 2006). Annual surveys of the distribution of eggs and pelagic larvae (e.g., Moriondo-Danovaro, 2011) are not informative about post-larval drift and connectivity, as they are conducted during the summer (spawning season) and concentrate on spawning grounds. On the other hand, all developmental stages from eggs to juveniles have been found in the main spawning grounds (Moriondo-Danovaro, 2011). Thus, factual evidence supports a conceptual model in which coastal areas to the north and south of SJG function both as spawning and nursery grounds, implying potential for larval retention associated with two frontal systems that differ from each other in many respects.

While factual evidence of connectivity between major spawning/nursery areas is lacking, mark-recapture data (Roux et al., 2012) and tracking of migrating shrimp by the fleet consistently support asymmetric connectivity, with a predominantly northward direction of shrimp leaving the south SJG closed area. The origin of the shrimp concentrating at the northern end of the Outer SJG front between November and January remains unknown. A likely hypothesis is that they correspond to shrimp migrating off the spawning/nursery ground associated with the North SJG front. The concentration is observed before shrimp start to leave the South SJG front region in February. As indicated earlier, spawning occurs earlier in the north than in the south of SJG, and juveniles presumably grow faster in the latter due to the higher temperature.

5.5. Final remarks

Based on integration of our synoptic results on surface oceanography and fleet behavior with prior information on regional oceanography and shrimp biology, we propose a conceptual model in which the North and South SJG fronts, symmetrically located along the northern and southern coasts of SJG, harbor the main spawning/nursery grounds sustaining the SJG red shrimp stock. While both the North and South SJG fronts constitute triads in the sense of Bakun (2010), they are radically different from each other in many respects. The thermohaline South SJG front has its maximum expression during the winter, reflecting the influence of the Magellanic Plume, while the North SJG front develops during spring and summer as the water column becomes stratified in the central basin of the gulf. Wind-related down-welling inshore of the front prevails in the North SJG, and upwelling in the South SJG frontal area. Chlorophyll *a* is concentrated near the thermocline on the stratified side of the North SJG, and for that reason it is not detected by remote sensors during the spring bloom and the summer, but becomes apparent offshore from the summer position of the front when the thermocline deepens during fall (May). In the South SJG front Chl-a concentration is apparent inshore from the front all year-round, related in part to upwelling-mediated resuspension.

The SJG ecosystem, as we see it today, took shape during the last post-glacial, as an endorheic depression was flooded *ca.* 15,500 calibrated years BP (Ponce et al., 2011, his Fig. 6), a short time-frame in terms of life-history evolution. One implication that red shrimp life history is not likely to have evolved to match present hydrographic scenarios. Its extraordinary productivity is due to a degree of plasticity that facilitates the use of the triadic configurations contingently available in the region, despite them differing from each other in significant properties and dynamics. Such plasticity is potentially significant for the resilience of the stock in the face of climate change (Koeller et al., 2009).

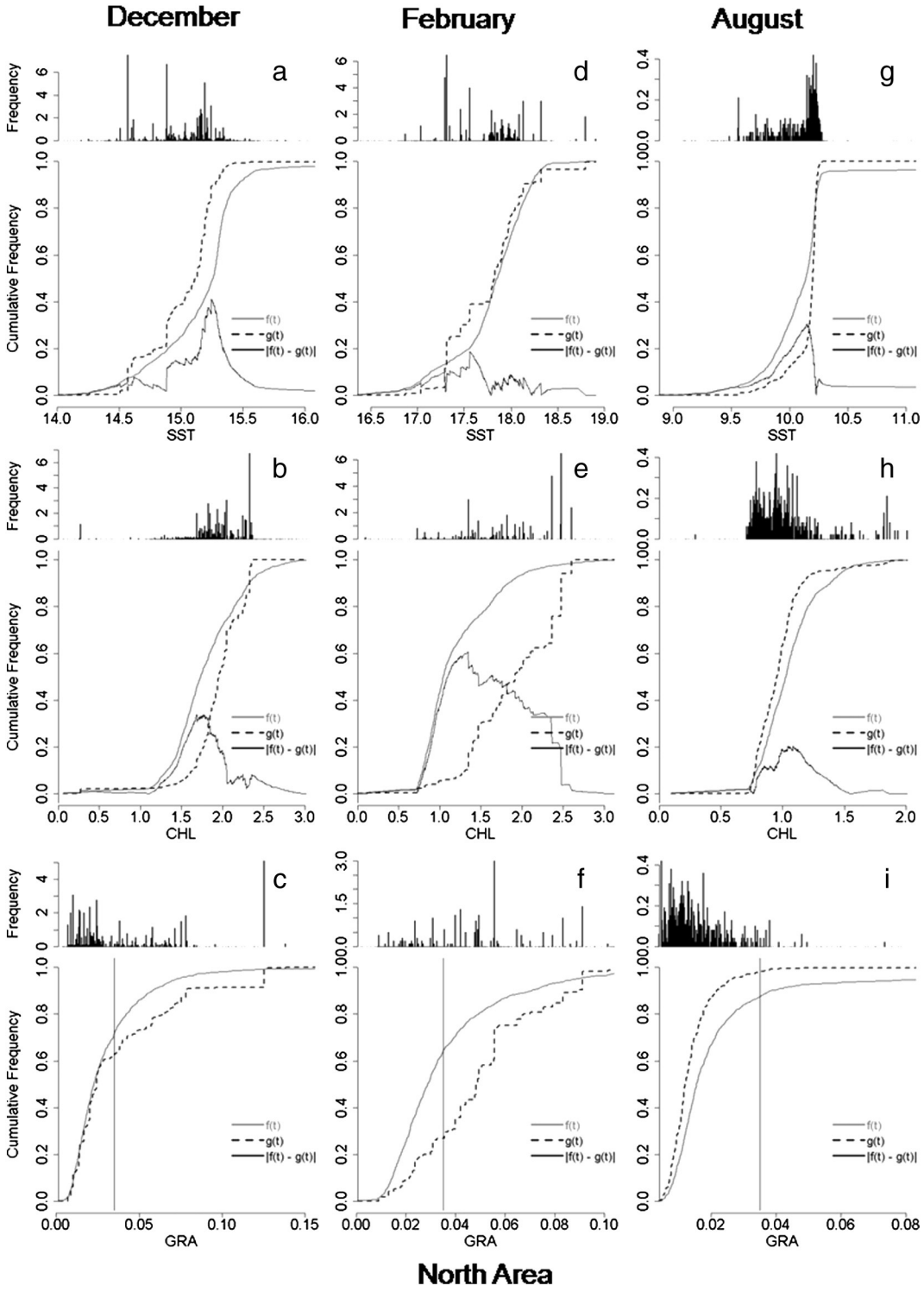

Fig. 7. Ibid, Fig. 6, north sector of San Jorge Gulf.

The SJG red shrimp fishery (and its northward extension to the Rawson grounds) has remained productive for two decades despite the lack of a management strategy supported by regular stock assessments. Closures of the Mazarredo spawning/nursery since 1985 and of the Inter-jurisdictional Marine Park since 2006 may be key to the continued productivity of the stock. Carl Walters (quoted by Orensanz and Jamieson, 1998) claimed that "if we look at fisheries that have been successful over the long term, the reason for their success is not to be found in assessment, learning and management models, but in the existence of a spatial accident, something about the spatial structure of population dynamics interacting with regulatory systems, or about the behavior of the species and fishers, that creates a large scale refuge for a substantial segment of the spawning population." Following up, Orensanz et al. (1998) prescribed that "when such 'natural accidents' do not exist, the first priority of any sensible management plan should be to create their equivalents: reproductive refugia that, through regulation and enforcement, are off limits to fishery operations." This, we argue, provides the rationale for keeping and refining reproductive refugia associated with the North and South SJG fronts in the Patagonian red shrimp fishery (Góngora et al., 2012).

Acknowledgments

The authors thank M. Sapoznik, N. Pérez de la Torre and M.R. Marin for their assistance in the processing of satellite images; Noela Sánchez-Carnero for her critical review and suggested changes to the manuscript. Thorough reading and thoughtful criticism from two anonymous reviewers contributed to significant improvement of the manuscript. Nora Glembocki and Gabriela Williams were supported by fellowships of CONICET (Argentina), and the work was partially supported by the projects PICT 2003 N° 15221, 2006 N° 1575, 2006 N° 649 (ANPCyT, Argentina), SAOCOM 2012 N° 14 CONAE (Comisión Nacional de Actividades Espaciales). This contribution is part of the doctoral thesis of Nora Glembocki.

Appendix A. Supplementary data

Supplementary data to this article can be found online at http://dx.doi.org/10.1016/j.seares.2014.10.011.

References

Acha, E.M., Mianzan, H.W., Guerrero, R.M., Favero, M., Bava, J., 2004. Marine fronts at the continental shelves of austral South American physical and ecological processes. J. Mar. Syst. 44, 83–105. http://dx.doi.org/10.1016/j.jmarsys.2003.09.005.

Akselman, R., 1996. Estudios ecológicos en el golfo San Jorge y adyacencias (Atlántico Sudoccidental). Distribución, abundancia y variación estacional del fitoplancton en relación a factores fisico-químicos y la dinámica hidrológica(PhD. diss.) Universidad de Buenos Aires, Facultad de Ciencias Exactas y Naturales, Argentina (234 pp.).

Alemany, D., Acha, E.M., Iribarne, O.O., 2014. Marine fronts are important fishing areas for demersal species at the Argentine Sea (Southwest Atlantic Ocean). J. Sea Res. 87, 56–67.

Amoroso, R.O., Parma, A.M., Orensanz, J.M., Gagliardini, D.A., 2011. Zooming the macroscope: medium-resolution remote sensing as a framework for the assessment of a small-scale fishery. ICES J. Mar. Sci. 68, 696–706.

Bakun, A., 2010. Linking climate to population variability in marine ecosystems characterized by non-simple dynamics: conceptual templates and schematic constructs. J. Mar. Syst. 79, 361–373. http://dx.doi.org/10.1016/j.jmarsys.2008.12.008.

Bava, J., 2004. Metodologías de procesamiento de imágenes NOAA-AVHRR y su utilización en aplicaciones oceanográficas y biológico-pesqueras en el Atlántico Sudoccidental(PhD. diss.) Universidad de Buenos Aires, Facultad de Ciencias Exactas y Naturales, Argentina (215 pp.).

Belkin, I.M., Cornillon, P.C., Sherman, K., 2009. Fronts in large marine ecosystems. Prog. Oceanogr. 81, 223–236. http://dx.doi.org/10.1016/j.pocean.2009.04.015.

Beron-Vera, F.J., Ripa, P., 2000. Three-dimensional aspect of the seasonal heat balance in the Gulf of California. J. Geophys. Res. 105, 11441–11457. http://dx.doi.org/10.1029/2000JC900038.

Bogazzi, E., Baldoni, A., Rivas, A., Martos, P., Reta, R., Orensanz, J.M., Lasta, M., Dell'Arciprete, P., Werner, F., 2005. Association between areas of concentration of Patagonian scallop (*Zygochlamys patagonica*) and frontal systems in the south-western Atlantic. Fish. Oceanogr. 14, 359–376. http://dx.doi.org/10.1111/j.1365-2419.2005.00340.x.

Boschi, E.E., 1989. Biología Pesquera del Langostino del Litoral Patagónico de Argentina (*Pleoticus muelleri*). Serie Contribuciones del INIDEP. Contribución N° 646. Instituto Nacional de Desarrollo Pesquero (INIDEP), (72 pp. Mar del Plata, Available at http://www.sidalc.net/docau.htm, last accessed 10 Ocober 2013).

Boschi, E.E., 1997. Las pesquerías de crustáceos decápodos en el litoral de la República Argentina. Investig. Mar. 25, 19–40. http://dx.doi.org/10.4067/S0717-71781997002500003 (last accessed 10 Ocober 2013).

Carreto, J.I., Carignan, M.O., Montoya, N.G., Cucchi Colleoni, D.A., 2007. Ecología del fitoplancton en los sistemas frontales del mar argentino. In: Carreto, J.I., Bremec, C. (Eds.), El Mar Argentino y sus recursos PesquerosEl ambiente Marino Tomo V. INIDEP, Mar del Plata (169 pp. Available at http://www.sidalc.net/docau.htm, last accessed 10 Ocober 2013).

Criales, M.M., Robblee, M.B., Browder, J.A., Cardenas, H., Jackson, T.L., 2011. Field observations on selective tidal stream transport for postlarval and juvenile pink shrimp in Florida. J. Crustac. Biol. 31, 26–33. http://dx.doi.org/10.1651/10-3291.1.

Cucchi Colleoni, A.D., Carreto, J.I., 2001. Variación estacional de la biomasa fitoplanctónica en el golfo San Jorge. Resultados de las campañas de investigación: OB-01/00, OB-03/00, OB-10/00, y OB-12/00. Informe Técnico Interno N°49, (30 pp., Available at http://www.sidalc.net/docau.htm, last accessed 10 October 2013).

Evans, G.T., Parslow, J.S., 1985. A model of annual plankton cycles. Biol. Oceanogr. 3, 327–347.

Fernández, M., 2006. Características físico-químicas de los sedimentos del golfo San Jorge y su relación con los organismos bentónicos del sector(PhD. diss.) Universidad Nacional de Mar del plata, Facultad de Ciencias Exactas, Argentina (308 pp., Available at http://www.sidalc.net/docau.htm, last accessed 10 Ocober 2013).

Fernández, M., Roux, A., Fernández, E., Caló, J., Marcos, A., Aldacur, H., 2003. Grain-size analysis of surficial sediments from Golfo San Jorge, Argentina. J. Mar. Biol. Assoc. UK 83, 1193–1197. http://dx.doi.org/10.1017/S0025315403008488.

Fernández, M., Carreto, J.I., Mora, J., Roux, A., 2005. Physico-chemical characterization of the benthic environment of the golfo San Jorge, Argentina. J. Mar. Biol. Assoc. UK 85, 1317–1328. http://dx.doi.org/10.1017/S002531540501249X.

Fernández, M., Mora, J., Roux, A., Cucchi-Colleoni, A.D., Gasparoni, J.C., 2008. New contribution on spatial and seasonal variability of environmental conditions of the golfo San Jorge benthic system, Argentina. J. Mar. Biol. Assoc. UK 88, 227–236. http://dx.doi.org/10.1017/S0025315408000465.

Fernández, M., Iorio, M.I., Hernández, D., Macchi, G., 2012. Studies on the reproductive dynamics of *Pleoticus muelleri*(Bate, 1888) (Crustacea, Decapoda, Solenoceridae) of Patagonia, Argentina. Lat. Am. J. Aquat. Res. 40, 858–871. http://dx.doi.org/10.3856/vol40-issue4-fulltext-4.

Findlay, H.S., Yool, A., Nodale, M., Pitchford, J.W., 2006. Modelling of autumn plankton bloom dynamics. J. Plankton Res. 28, 209–220.

Fischbach, C., 1993. Ecología larval del langostino (*Pleoticus muelleri*). Algunos aspectos de la dinámica de los estadios planctónicos en el litoral bonaerense (Argentina). Frente Marít. 14A, 101–109 (Available at http://www.sidalc.net/docau.htm, last accessed 10 Ocober 2013).

Fischbach, C., De la Garza, J., Bertuche, D., 2006. La pesquería del langostino patagónico en el período 1991-2005. Informe Técnico Interno 03/06. Instituto Nacional de Investigación y Desarrollo Pesquero (INIDEP), Mar del Plata, p. 21.

Foley, M.M., Halpern, B.S., Micheli, F., Armsby, M.H., Caldwell, M.R., Crain, C.M., Prahler, E., Rohr, N., Sivas, D., Beck, M.W., Carr, M.H., Crowder, L.B., Duffy, E., Hacker, S.D., McLeod, K.L., Palumbi, S.R., Peterson, C.H., Regan, H.M., Ruckelshaus, M.H., Sandifer, P.A., Steneck, R.S., 2010. Guiding ecological principles for marine spatial planning. Mar. Policy 34, 955–966. http://dx.doi.org/10.1016/j.marpol.2010.02.001.

Gagliardini, D.A., Amoroso, R.O., Dell' Arciprete, P.O., Yorio, P., Orensanz, J.M., 2004. Detection of small-scale coastal oceanographic processes through Landsat-TM/ETM + images: implications for the study of biological processes along Patagonian coasts of Argentina. Int. J. Biodivers. Oceanol. Conserv. 68, 194–200. http://dx.doi.org/10.4067/S0717-65382004000200035.

Gerritsen, H., Lordan, C., 2011. Integrating vessel monitoring systems (VMS) data with daily catch data from logbooks to explore the spatial distribution of catch and effort at high resolution. ICES J. Mar. Sci. 68, 245–252. http://dx.doi.org/10.1093/icesjms/fsq137.

Glorioso, P.D., Flather, R.A., 1995. A barotropic model of the currents off SE South America. J. Geophys. Res. 100, 13427–13440. http://dx.doi.org/10.1029/95JC00942.

Góngora, M.E., 2011. Dinámica y manejo de la captura incidental de peces en la pesquería del langostino patagónico (*Pleoticus muelleri*)(PhD. diss) Universidad Nacional de Comahue, Bariloche, Argentina (224 pp., Available at http://oceandocs.net/handle/1834/4190, last accessed 10 Ocober 2013).

Góngora, M.E., Gonzalez Zevallos, D., Pettovello, A., Mendia, L., 2012. Caracterización de las principales pesquerías del golfo San Jorge, Patagonia, Argentina. Lat. Am. J. Aquat. Res. 40, 1–11. http://dx.doi.org/10.3856/vol40-issue1-fulltext-1.

Grant, J., Cranford, P., Emerson, C., 1997. Sediment resuspension rates, organic matter quality and food utilization by sea scallops (*Placopecten magellanicus*) on Georges Bank. J. Mar. Res. 55, 965–994. http://dx.doi.org/10.1357/0022240973224193.

Holman, R., Haller, M.C., 2013. Remote Sensing of the nearshore. Annu. Rev. Mar. Sci. 5, 95–113. http://dx.doi.org/10.1146/annurev-marine-121211-172408.

Iorio, M.I., Scelzo, M.A., Boschi, E.E., 1990. Desarrollo larval y postlarval del langostino *Pleoticus muelleri* Bate 1888 (Crustacea, Decapoda, Solenoceridae). Sci. Mar. 54, 329–341.

Klemas, V., 2012. Fisheries Applications of Remote Sensing: An Overview. Fish. Res. http://dx.doi.org/10.1016/j.fishres.2012.02.027.

Koeller, P., Fuentes-Yaco, C., Platt, T., Sathyendranath, S., Richards, A., Ouellet, P., Orr, D., et al., 2009. Basin-scale coherence in phenology of shrimps and phytoplankton in the North Atlantic Ocean. Science 324, 791–793.

McClain, E.P., Pichel, W.G., Walton, C.C., 1985. Comparative performance of AVHRR based multichannel sea surface temperature. J. Geophys. Res. 90, 11587–11601.

Moriondo-Danovaro, P.I., 2011. Distribución y abundancia de huevos y larvas de langostino patagónico (*Pleoticus muelleri*) (PENAEOIDEA, SOLENOCERIDAE) en las temporadas estivales de 2008 y 2009. Informe Técnico 83. Instituto Nacional de Investigación y Desarrollo Pesquero (INIDEP), Mar del Plata (Argentina) (20 pp., Available at http://www.oceandocs.org/handle/1834/4880, last accessed 10 Ocober 2013).

Nievas, M.L., Esteves, J.L., 2007. Relevamiento de actividades relacionadas con la explotación de petróleo en zona costera patagónica y datos preliminares sobre residuos de hidrocarburos en puertos. Informe Técnico. Fundación Patagonia Natural, Puerto Madryn (Argentina) (68 pp., Available at http://www.patagonianatural.org/attachments/156_Informe%20tecnico%20N%C2%BA1.pdf, last accessed 10 Ocober 2013).

Ocampo Reinaldo, M., González, R., Williams, G., Storero, L.P., Romero, M.A., Narvarte, M., Gagliardini, D.A., 2013. Spatial patterns of the Argentine hake *Merluccius hubbsi* and Oceanographic processes in a semi-enclosed Patagonian ecosystem. Mar. Biol. Res. 9, 394–406. http://dx.doi.org/10.1080/17451000.2012.739700.

O'Reilly, J.E., Maritorena, S., Mitchell, B.G., Siegel, D.A., Carder, K.L., Garver, S.A., Kahry, M., McClain, C., 1998. Ocean color chlorophyll algorithms for SeaWiFS. J. Geophys. Res. 103, 24937–24953.

O'Reilly, J.E., Maritorena, S., Siegel, D.A., O'Brien, M.C., Toole, D., Mitchell, B.G., Kahru, M., Cota, G.F., Carder, K.L., Muller-karger, F., Harding, L., Magnuson, A., Phinney, D., Moore, G.F., Aiken, J., Arrigo, K.R., Letelier, R., Culver, M., 2000. Ocean Color Chlorophyll a Algorithms for SeaWiFS, OC2 and OC4: Version 4 Chapter 2. SeaWiFS Postlaunch Calibration and Validation Analyses, Part 3.

Orensanz, J.M., Jamieson, G.S., 1998. The assessment and management of spatially structured stocks. Can. Spec. Publ. Fish. Aquat. Sci. 125, 441–459.

Orensanz, J.M., Armstrong, J., Armstrong, D.A., Hilborn, R., 1998. Crustacean resources are vulnerable to serial depletion- The multifaceted decline of shrimp and crab fisheries in the greater Gulf of Alaska. Rev. Fish Biol. Fish. 8, 117–176.

Palma, E.D., Matano, R.P., 2012. A numerical study of the Magellan Plume. J. Geophys. Res. 117, C05041. http://dx.doi.org/10.1029/2011JC007750.
Palma, E.D., Matano, R.P., Piola, A.R., 2004. A numerical study of the southwestern Atlantic shelf circulation. Part I: The barotropic response to tidal and wind forcing. J. Geophys. Res. 109, C08014. http://dx.doi.org/10.1029/2004JC002315.
Palma, E.D., Matano, R.P., Piola, A.R., 2008. A numerical study of the Southwestern Atlantic Shelf circulation: Stratified ocean response to local and offshore forcing. J. Geophys. Res. 113, C11010. http://dx.doi.org/10.1029/2007JC004720.
Perry, R.I., Smith, S.J., 1994. Identifying habitat associations sf marine fishes using survey data: an application to the northwest Atlantic. Can. J. Fish. Aquat. Sci. 51, 589–602.
Ponce, J.F., Rabassa, J., Coronato, A., Borromei, A.M., 2011. Palaeogeographical evolution of the Atlantic coast of Pampa and Patagonia from the last glacial maximum to the Middle Holocene. Biol. J. Linn. Soc. 103, 363–379.
R Core Team, 2013. R: A language and environment for statistical computing. R Foundation for Statistical Computing, Vienna, Austria (Available at http://www.R-project.org, last accessed 10 October 2013).
Rivas, A.L., 2006. Quantitative estimation of the influence of surface thermal fronts over chlorophyll concentration at the Patagonian shelf. J. Mar. Syst. 63, 183–190.
Rivas, A.L., 2010. Spatial and temporal variability of satellite-derived sea surface temperature in the southwestern Atlantic Ocean. Cont. Shelf Res. 30, 752–760. http://dx.doi.org/10.1016/j.csr.2010.01.009.
Rivas, A.L., Pisoni, J.P., 2010. Identification, characteristics and seasonal evolution of surface thermal fronts in the Argentinean continental shelf. J. Mar. Syst. 79, 134–143. http://dx.doi.org/10.1016/j.jmarsys.2009.07.008.
Rivas, A.L., Dogliotti, A.I., Gagliardini, D.A., 2006. Seasonal variability in satellite-measured surface chlorophyll in the Patagonian Shelf. Cont. Shelf Res. 26, 703–720. http://dx.doi.org/10.1016/j.csr.2006.01.013.
Rothlisberg, P.C., Church, J.A., Fandry, C.B., 1995. Mechanism for near-shore concentration and estuarine recruitment of post-larval *Penaeus plebejus* Hess (Decapoda, Penaeidae). Estuar. Coast. Shelf Sci. 40, 115–138.
Roux, A.M., de la Garza, J.L., Piñero, R., Bertuche, D., 2012. La ruta de migración del langostino patagónico. Informe Técnico. Instituto Nacional de Investigaciones y Desarrollo Pesquero (INIDEP), Mar del Plata, Argentina (24 pp., Available at http://www.sidalc.net/docau.htm, last accessed 10 October 2013).
Russo, T., Parisi, A., Garofalo, G., Gristina, M., Cataudella, S., Fiorentino, F., 2014. SMART: A spatially explicit bio-economic model for assessing and managing demersal fisheries, with an application to Italian trawlers in the Strait of Sicily. PLoS ONE 9 (1), e86222. http://dx.doi.org/10.1371/journal.pone.0086222.
Simpson, J.J., 1990. On the accurate detection and enhancement of oceanic features observed in satellite data. Remote Sens. Environ. 33, 17-3. http://dx.doi.org/10.1016/0034-4257(90)90052-N.
Tonini, M., Palma, E., Rivas, A.L., 2006. Modelo de alta resolución de los golfos norpatagónicos. Mecánica Comput. XXV, 1441–1460 (Available at http://www.amcaonline.org.ar).
Wenner, E.L., Knott, D.M., Barans, C.A., Wilde, S., Blanton, J.O., Amft, J., 2005. Key factors influencing transport of white shrimp (*Litopenaeus setiferus*) post-larvae into the Ossabaw Sound system, Georgia, USA. Fish. Oceanogr. 14, 175–194. http://dx.doi.org/10.1111/j.1365-2419.2005.00328.x.
Williams, G., Sapoznik, M., Ocampo-Reinaldo, M., Solis, M., Narvarte, M., González, R., Esteves, J.L., Gagliardini, D.A., 2010. Comparison of AVHRR and SeaWiFS imagery with fishing activity and in situ data in San Matias Gulf, Argentina. Int. J. Remote Sens. 31, 4531–4542. http://dx.doi.org/10.1016/j.csr.2012.08.014.
Woillez, M., Poulard, J.-C., Rivoirard, J., Petitgas, P., Bez, N., 2007. Indices for capturing spatial patterns and their evolution in time, with application to European hake (*Merluccius merluccius*) in the Bay of Biscay. ICES J. Mar. Sci. 64, 537–550.
Yorio, P., 2001. Antecedentes para la creación de una nueva área marina protegida en la Provincia de Chubut: el norte del golfo San Jorge. Documento Técnico. Centro Nacional Patagónico, Puerto Madryn (Argentina) (27 pp.).
Zar, J.H., 1999. Biostatistical Analysis, 4th ed. Prentice Hall, Englewood Cliffs, NJ.